Distribution of Pb, Zn, Fe, As, Sn, Sb, Bi and Ni between oxide liquid and metal in the "CuO$_{0.5}$"-CaO-AlO$_{1.5}$ system in equilibrium with Cu metal at 1400 °C.

G. Khartcyzov[1], M. Shevchenko[2] and E. Jak[3]

1. PhD candidate, Pyrosearch, School of Chemical Engineering, the University of Queensland, Brisbane QLD 4072. Email: g.khartcyzov@uq.edu.au
2. Research fellow, Pyrosearch, School of Chemical Engineering, the University of Queensland, Brisbane QLD 4072. Email: m.shevchenko@uq.edu.au
3. Professor, Pyrosearch, School of Chemical Engineering, the University of Queensland, Brisbane QLD 4072. Email: e.jak@uq.edu.au

ABSTRACT

The increasing complexity of ore resources and recycled materials in the feed of pyrometallurgical processes present a technical challenge to the metallurgical engineers working on maximizing the recovery of the valuable elements and minimizing the environmental impact of the processes. To address this challenge, the availability of computational tools that can predict the mass and energy balance in complex systems is required. Then the accurate description of phase equilibria in the complex multicomponent systems describing the chemistry of the pyrometallurgical processes becomes critical for the correct implementation of the indicated tools and facing the outlined industrial challenges.

In the present study the distribution of selected elements (Pb, Zn, Fe, As, Sn, Sb, Bi and Ni) between oxide liquid and metal in the "CuO$_{0.5}$"-CaO-AlO$_{1.5}$ system in equilibrium with Cu metal at 1400 °C (liquidus of CaAl$_2$O$_4$) was experimentally studied using the equilibration and quenching technique followed by the electron probe X-ray microanalysis of the resulted samples. The study covered a wide range of effective p(O$_2$) over the system from 10^{-11} to $10^{-3.5}$ (corresponding to formation of immiscible CuO$_{0.5}$-rich slag). To avoid loss of volatile elements (Pb, Zn, As, Sn, Sb and Bi), a correlation between "CuO$_{0.5}$" in oxide liquid and p(O$_2$) in open system was obtained first, followed by studying the volatile elements distribution in closed conditions (Al$_2$O$_3$ crucible sealed in SiO$_2$ ampoule), where "CuO$_{0.5}$" concentration was used as a marker to evaluate the effective p(O$_2$) over the system.

The experimental results were then used for the optimisation of the thermodynamic model parameters of the system as part of the integrated experimental and self-consisting thermodynamic modelling research program of phase equilibria in the Cu-Pb-Zn-Fe-Ca-Si-Al-Mg-O-S-(As, Sn, Sb, Bi, Ag, Au, Ni, Cr, Co and Na) gas/oxide liquid/matte/speiss/metal/solids system.

INTRODUCTION

The recycling of nonferrous metals, an essential component for sustainable development, faces significant challenges due to the variability of the feedstock and the complex chemistry of the elements involved (Loibl and Tercero Espinoza, 2021). The development of new processes and the optimization of existing processes require computational tools capable of predicting phase equilibria, energy balance and partitioning of all chemical elements. In turn, the accuracy of the predictions is improved by the integrated experimental and thermodynamic modelling study of the chemical system characterising the process of interest. The present study focuses on the distribution of the Cu, Pb, Zn, Fe, As, Sn, Sb, Bi and Ni between the oxide liquid and metallic phases of the "CuO$_{0.5}$"-CaO-AlO$_{1.5}$ system to help describe the complex phase equilibria in non-ferrous recycling slags.

The present study is a part of a broader research program supported by an international consortium of copper, lead, zinc and iron producing companies and focused on the integrated experimental and thermodynamic modelling study of phase equilibria in the Cu-Pb-Zn-Fe-Ca-Si-Al-Mg-O-S-(As, Sn, Sb, Bi, Ag, Au, Ni, Cr, Co and Na) gas/oxide liquid/matte/speiss/metal/solids system, and the development of a self-consistent set of the thermodynamic parameters for the described system

(Shevchenko et al., 2021, Shishin et al., 2018, Shishin et al., 2019). The new experimental data on the presented subsystems will enable these and the larger multicomponent systems to be described using chemical thermodynamic models. Phase equilibria data and other thermodynamic properties of these systems will then provide an important foundation for the improved understanding and, importantly, prediction of the behaviour of these slags in the industrial processes.

Similar works were found in the literature studying the distribution of the different elements in the iron silicate (Yazawa, 1981, Hidayat et al., 2021), iron alumina silicate (Nagamori and Mackey, 1977), iron calcium silicate (Anindya et al., 2013, Anindya et al., 2014) and calcium ferrite (Yazawa, 1981) slags. The present work is considered to be the first to study the distributions of Cu, Pb, Zn, Fe, As, Sn, Sb, Bi and Ni in the calcium aluminate slags.

Figure 1 demonstrates the liquidus projection diagram of the "$CuO_{0.5}$"-CaO-$AlO_{1.5}$ system in equilibrium with metallic copper calculated using the FactSage software (Bale et al., 2016) and internal thermodynamic database (Shevchenko et al., 2021, Shishin et al., 2018, Shishin et al., 2019) with the area of the interest for the present study highlighted on the diagram. This area was chosen for several reasons: 1) it is located in the low-temperature region of the diagram, 2) it covers the range of concentrations of "$CuO_{0.5}$" in the oxide liquid (wide range of oxygen partial pressures), and 3) the $CaAl_2O_4$-$AlO_{1.5}$ side of the CaO-$AlO_{1.5}$ system promotes the formation of the layer of calcium aluminates on the Al_2O_3 crucible or Al_2O_3-based refractory material for all corresponding bulk compositions. These reasons make the chosen area suitable and beneficial for the possible WEEE (waste electronic and electrical equipment) recycling processes.
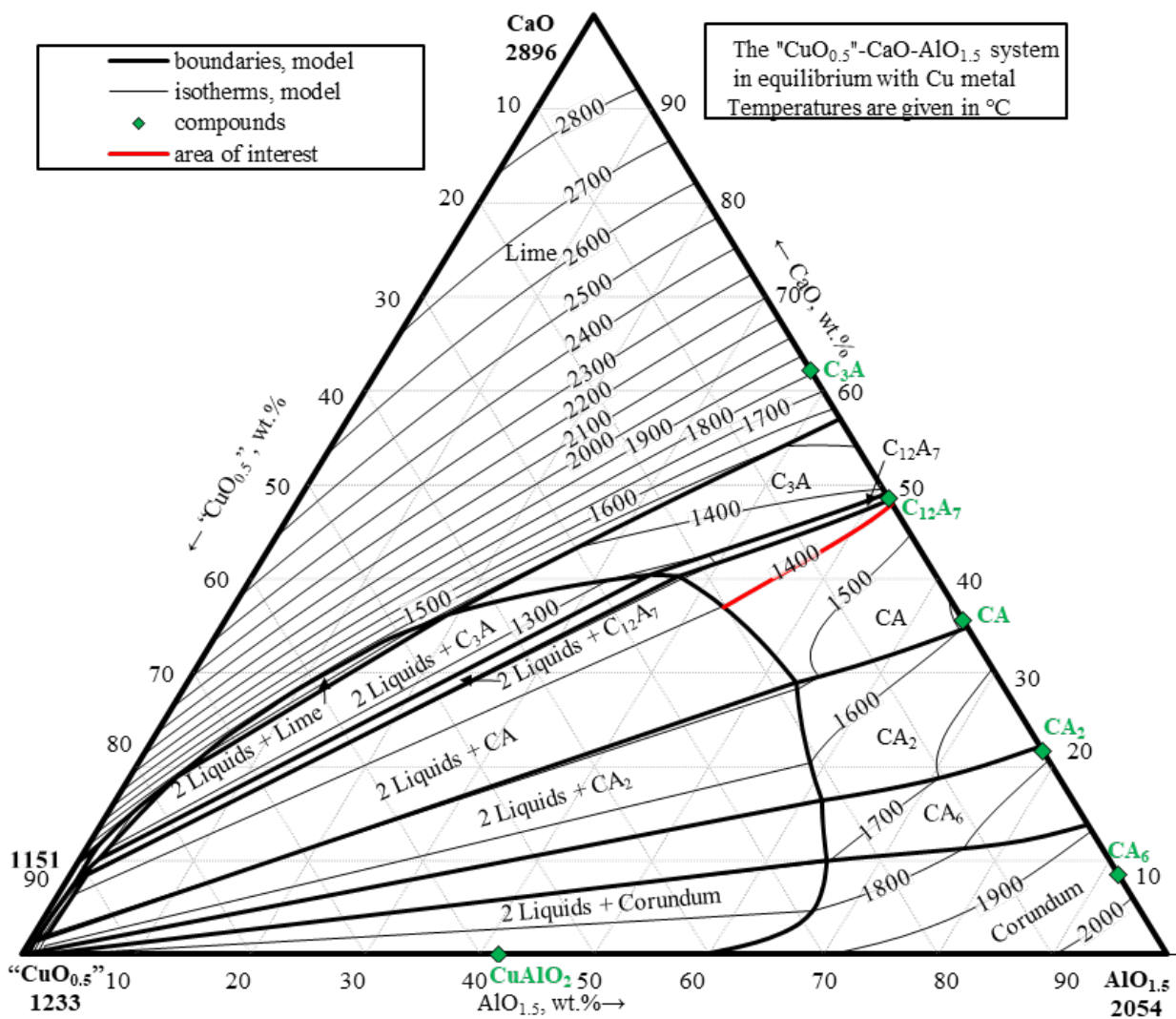

Figure 1. Calculated phase diagram of the "$CuO_{0.5}$"-CaO-$AlO_{1.5}$ system in equilibrium with Cu metal with highlighted area of interest for the present study.

The present study provides the experimental description of the phase equilibria in the "$CuO_{0.5}$"-CaO-$AlO_{1.5}$-(Pb, Zn, Fe, As, Sn, Sb, Bi and Ni) system in equilibrium with metallic phase and $CaAl_2O_4$ at 1400 °C, including: 1) correlation between the concentration of copper oxide in the "$CuO_{0.5}$"-CaO-$AlO_{1.5}$ oxide liquid in equilibrium with $CaAl_2O_4$ at 1400 °C and effective oxygen partial pressure ($p(O_2)$) over the system, and 2) the distributions of the Cu, Pb, Zn, Fe, As, Sn, Sb, Bi and Ni among the oxide liquid and the metallic phase in the "$CuO_{0.5}$"-CaO-$AlO_{1.5}$ system in equilibrium with $CaAl_2O_4$ at 1400 °C in the wide range of oxygen partial pressures from 10^{-11} to $10^{-3.5}$.

RESEARCH METHODOLOGY

The experimental procedure and apparatus used in the present study were described earlier by the authors (Jak et al., 1995, Jak, 2012, Khartcyzov et al., 2022, Khartcyzov et al., 2023). The initial mixtures were made of high-purity Cu_2O, ZnO, Fe_2O_3 and Al_2O_3 (all ≥99.9 wt.% purity, supplied by Alfa Aesar, MA, USA or by Sigma-Aldrich, MO, USA) oxide and Cu, Pb, Sn, Sb, Bi and Ni (≥99.9 wt.% purity; supplied by Alfa Aesar, MA, USA) metallic powders. As was added to the mixture in a form of Cu_3As (prepared by heating Cu and As powders at 5 °C/min to 900 °C (with 1 hour hold at 300, 500, 700 and 800 °C) and keeping over 2 hours, then allowing to cool with the furnace). CaO was added to the mixture in a form of the "master slag" CaO-$AlO_{1.5}$, 55:45 molar ratio, prepared in advance by high-temperature sintering of mixed $CaCO_3$ and Al_2O_3 powders (≥99.9 wt.% purity; supplied by Alfa Aesar, MA, USA). About 0.5 g of mixture was used in each equilibration experiment. The initial compositions of the mixtures were selected so that $CaAl_2O_4$ was present in equilibrium with liquid slag and metals. The initial predictions of the targeted phase compositions were made for every sample using FactSage® 8.2 software (Bale et al., 2009, Bale et al., 2016) and continuously updated internal thermodynamic database (Shevchenko et al., 2021, Shishin et al., 2018, Shishin et al., 2019). The volume fraction of solids in the final sample after equilibration was targeted to be in the range from 10 to 50%, and preferably about 10%. Low proportion of solids ensures faster equilibration time, and facilitates quenching of liquid slag into amorphous material without change in composition. Solid phases acted as heterogeneous nucleation centres, so that a minimum distance of 10-20 μm between solid grains was necessary to ensure that an amorphous slag of uniform composition, unaffected by dendritic crystal growth during quenching, was obtained. The correlation between the proportion of the solid phases present in equilibrium and the distance between solid grains was described previously by the authors (Khartcyzov et al., 2022). An iterative procedure involving preliminary experiments was required to achieve the targeted phase proportions for a given equilibration temperature and bulk slag composition, since the exact liquidus compositions at a given temperature were not initially known. Homogenous slag areas, not affected by the growth of the "quench crystals", were analysed and included in the present study.

The mixtures were pressed into pellets using a tool steel die before being mounted on a substrate. Alumina crucibles (1.5 cm long, 1 cm outer diameter, 99.7 wt.% purity, supplied by Xiamen Wintrustek Advance Materials Co., LTD, China) were used as sample support substrates for equilibration. For the closed system experiments the alumina crucibles were additionally sealed inside silica ampoules (5 cm long, 1.3 cm outer diameter, 99.999%, supplied by GY, Jiangsu, China) to prevent the contamination of the samples with the suspension support materials and to limit the evaporation of the volatile species from the melt. The ceramic crucibles were previously found to be reliable as substrates (Khartcyzov et al., 2022, Hidayat et al., 2012, Chen et al., 2020). The precipitation of the primary phase on the ceramic substrate prevents the excessive dissolution of the substrate material into the slag ensuring little change in the bulk composition of the system during the equilibration time (Shevchenko and Jak, 2020, Klemettinen et al., 2017).

Each equilibration experiment was carried out in an electrical-resistance heated vertical tube furnace with an impervious recrystallized alumina (30-mm inner diameter) reaction tube with silicon carbide (SiC) heating element; the upper temperature limit for the furnace operation was 1700 °C. The samples were placed immediately adjacent to a working thermocouple (type B) that was encased in a recrystallized alumina sheath in the uniform hot zone of the furnace to monitor the actual sample temperature. The working thermocouple was calibrated against a standard thermocouple (supplied by the National Measurement Institute of Australia, NSW, Australia). The overall absolute temperature accuracy of the experiment was estimated to be ±3 K.

3

The samples were suspended in the hot zone of the furnace by Kanthal support wire (Fe-Cr-Al alloy, 0.7 (Kanthal D) or 1-mm (Kanthal A-1) diameter; melting temperature 1500 °C; suitable for operating up to $p(O_2)$ = 1 atm; supplied by Vulcan Stainless, VIC, Australia). High purity CO and CO_2 gases (>99.995% purity, supplied by Coregas, NSW, Australia) were used for the open system experiments. The samples were then equilibrated at the final target temperature for the required time. For the open system experiments the $p(O_2)$ was maintained by an accurate control of the CO/CO_2 ratio in the gas flow phase using calibrated U-tube capillary flowmeters. The desired flowrates of gases, corresponding to the indicated $p(O_2)$ were calculated using FactSage 8.2® FactPS database (Bale et al., 2016) for the ideal gas phase. The accuracy of the oxygen potential was confirmed using a DS-type oxygen probe (supplied and calibrated by Australian Oxygen Fabricators, Melbourne, VIC, Australia). At the end of the equilibration process, the samples were released and rapidly quenched into $CaCl_2$ brine solution at -20 °C. Brine solution was chosen over water due to the higher cooling rates (Pizetta Zordão et al., 2019, Luty, 1992). The samples were then washed thoroughly in water and ethanol, dried on a hot plate, mounted in epoxy resin and cross-sectioned and polished using conventional metallographic techniques.

The cross-sectioned samples were examined by optical microscopy, carbon-coated, and the compositions of the phases were measured by EPMA using wavelength-dispersive detectors (JEOL 8200L EPMA; Japan Electron Optics Ltd., Tokyo, Japan) operated at 15 kV accelerating voltage and 20 nA probe current. The standard Duncumb–Philibert atomic number, absorption, and fluorescence (ZAF) correction supplied by JEOL (Philibert, 1963, Duncumb and Reed, 1968, Duncumb, 1971) was used. Copper (Cu) (for Cu and "$CuO_{0.5}$" measurements), zincite (ZnO) (for Zn and ZnO measurements), hematite (Fe_2O_3) (for Fe, FeO and $FeO_{1.5}$ measurements), wollastonite ($CaSiO_3$) (for CaO measurements), corundum (Al_2O_3) (for $AlO_{1.5}$ measurements), indium arsenide (InAs) (for As and $AsO_{1.5}$ measurements), cassiterite (SnO_2) (for Sn and SnO_2 measurements), antimony (Sb) (for Sb and $SbO_{1.5}$ measurements), bismuth (Bi) (for Bi and $BiO_{1.5}$ measurements) and nickel (Ni) (for Ni and NiO measurements) (supplied by Charles M. Taylor Co., Stanford, CA) and K456 lead-silica glass (71.4 wt% PbO) (for Pb and PbO) (supplied by NIST) were used as EPMA standards. The measurement uncertainties corresponded to the use of metals as standards for oxide measurements and vice versa did not exceed 0.2%. Only concentrations of metal cations were measured using EPMA; no data on the oxidation states of the metal cations in slag were obtained in the present study.

It was shown (Fallah-Mehrjardi et al., 2017) that the increase from fully focused electron beam (zero probe diameter) to 50 µm decreased the uncertainty of the copper slags compositions measured with EPMA and did not affect the accuracy of measurements. Thus, the probe diameter was selected depending on the size of the phase under investigation. The slag compositions reported in this study were measured mainly using 30 µm probe diameter, while the metallic phases were measured mainly with 50 to 100 µm probe diameters. The compositions of the phases reported in the present study are the average values of a number (from 15 to 25, usually 20) of independent measurements from different regions of the samples rather than single measurements.

The accuracy of the compositional measurements was improved using the standard JEOL ZAF correction following an approach similar to that described previously by the authors (Shevchenko and Jak, 2018, Shevchenko and Jak, 2017, Shevchenko et al., 2017, Shevchenko and Jak, 2019, Khartcyzov et al., 2022, Khartcyzov et al., 2023). This involved using stoichiometric compounds of known composition (Cu_2PbO_2, Ca_2CuO_3, $CuAlO_2$, $ZnAl_2O_4$, Ca_2PbO_4, $Ca_2Fe_2O_5$, $CaFe_2O_4$, $CaFe_4O_7$, $FeAl_2O_4$, $Ca_3Al_2O_6$, $CaAl_2O_4$, $CaAl_4O_7$) as secondary internal standards. The following equations (1-6) were then developed and applied to correct all cations concentrations in the target system of the present study:

$$x_{CuO_x}^{corrected} = x_{CuO_x}(1 - 0.0336x_{PbO} + 0.035x_{CaO} + 0.116x_{AlO_{1.5}}),$$ (1)

$$x_{ZnO}^{corrected} = x_{ZnO}(1 + 0.06x_{AlO_{1.5}}),$$ (2)

$$x_{PbO}^{corrected} = x_{PbO}(1 + 0.0336x_{CuO_x} + 0.0192x_{CaO}),$$ (3)

$$x_{FeO_x}^{corrected} = x_{FeO_x}(1 + 0.0208x_{CaO} + 0.0119x_{CaO}^2 - 0.0119x_{FeO_x}x_{CaO} + 0.038x_{AlO_{1.5}}),$$ (4)

$$x_{CaO}^{corrected} = x_{CaO}(1 - 0.035x_{CuO_x} - 0.0192x_{PbO}$$

$$-0.0208x_{FeO_x} - 0.0119x_{FeO_x}^2 + 0.0119x_{CaO}x_{FeO_x} - 0.044x_{AlO_{1.5}}),\qquad(5)$$

$$x_{AlO_{1.5}}^{corrected} = x_{AlO_{1.5}}(1 - 0.116x_{CuO_x} - 0.06x_{ZnO} - 0.038x_{FeO_x} + 0.044x_{CaO}),\qquad(6),$$

where x(CuO$_x$, PbO, ZnO, FeO$_x$, CaO, AlO$_{1.5}$) are the cation molar fractions after the standard JEOL ZAF corrections, and x(CuO$_x$, PbO, ZnO, FeO$_x$, CaO, AlO$_{1.5}$)^{corrected} are the corrected cation molar fractions respectively.

To ensure the achievement of equilibrium in the samples, the "4-point test" (Jak, 2012, Shevchenko et al., 2016) was used including: (1) variation of equilibration time; (2) assessment of the compositional homogeneity of the phases by EPMA; (3) approaching the final equilibrium point from different starting conditions; and, importantly, (4) consideration of reactions specific to this system that may affect the achievement of equilibrium or reduce the accuracy.

The presence of volatile elements (Pb, Zn, As, Sn, Sb and Bi) in the system made it impossible to run the equilibration experiments in the open system at the controlled p(O$_2$). To overcome this issue, the experimental methodology similar to the one described before by the authors (Hidayat et al., 2018) was developed and used in the present study. The methodology involves closed system experiments in the sealed ampoules using the Cu$_{metal}$/Cu$_2$O$_{slag}$ couple as internal measure of the effective p(O$_2$) over the system. In the presence of metallic Cu, the change in the oxidation potential of the system results in the change of the solubility of "CuO$_{0.5}$" in the slag phase, according to the following reactions (Hidayat et al., 2018):

$$2Cu_{metal} + O_{slag} \leftrightarrow Cu_2O_{slag}\qquad(7)$$

The Cu$_{metal}$/Cu$_2$O$_{slag}$ couple then reflects the effective p(O$_2$) of the slag phase as per the following reaction:

$$2Cu_{metal} + \tfrac{1}{2}O_{2\,gas} \leftrightarrow Cu_2O_{slag}\qquad(8)$$

According to reaction (8), it is possible to estimate the effective p(O$_2$) over the system based on the concentration of "CuO$_{0.5}$" in the oxide liquid, that is in equilibrium with Cu metal. The correlation between the p(O$_2$) over the system and the concentration of "CuO$_{0.5}$" in the oxide liquid for the system of interest is required. In the present study the following approach was used:

1) Establishing the correlation between "CuO$_{0.5}$"in oxide liquid and p(O$_2$) over the system for the volatile-free "CuO$_{0.5}$"-CaO-AlO$_{1.5}$ system in equilibrium with Cu metal using accurate experimental data obtained with the open-system gas equilibration technique in the composition area of interest.

2) Performing closed-system equilibration experiments for the "CuO$_{0.5}$"-CaO-AlO$_{1.5}$-(Pb, Zn, As, Sn, Sb, Bi and Ni) chemical system.

3) Deriving the effective p(O$_2$) over the system based on the experimental information obtained in the steps 1-3.

RESULTS AND DISCUSSION

Preliminary experiments were carried out to find the conditions of achievement of equilibrium using the "4-point test" (Jak, 2012, Shevchenko et al., 2016) including: (1) variation of equilibration time; (2) assessment of the compositional homogeneity of the phases by EPMA; (3) approaching the final equilibrium point from different starting conditions; and, importantly, (4) consideration of reactions specific to this system that may affect the achievement of equilibrium or reduce the accuracy. For open system experiments, equilibration time varied from 1 to 5 hours to ensure that no further reactions between the condensed and gaseous phases take place in the sample. Homogeneity of the phases was examined in different locations of the samples. When compositional trends were observed, results were rejected, and equilibration time was increased. The dissolution of the substrate material into the liquid which could have potentially affected phase equilibria in the system was found to be not a problem, because no compositional trends were observed for the samples after equilibration and the targeted phases were obtained. Final equilibration times for the open system experiments are given in Table 1. For the closed system experiments, the equilibration time varied from 3 to 16 hours: 3 hours of equilibration were found enough for all samples, while some were equilibrated for 16 hours to study the achievement of equilibria with time or for the experimental

convenience. Final equilibration times are listed in Table 1. For selected experiments, different starting compositions were used, or samples were preheated by 50 °C; the measured compositions of liquids agreed within the standard deviation of measurements.

The results of the experiments in the "$CuO_{0.5}$"-CaO-$AlO_{1.5}$ system in equilibrium with Cu metal in the controlled gas atmosphere were given in Table 1. The comparison of the discussed experimental results with the thermodynamic predictions of the current thermodynamic model (Shevchenko et al., 2021, Shishin et al., 2018, Shishin et al., 2019) was presented in Figure 2.

Table 1. Experimental results for the distribution of Cu, Pb, Zn, Fe, As, Sn, Sb, Bi, Ni between oxide liquid and metal phase in the "$CuO_{0.5}$"-CaO-$AlO_{1.5}$ system in equilibrium with $CaAl_2O_4$ at 1400 °C.

Element MeO_x/Me	Preheat Temperature, °C	Final	Time hour	Phases present	"$CuO_{0.5}$" / Cu	CaO / Ca	$AlO_{1.5}$ / Al	MeO_x / Me	Ox / Met	$Log_{10}L^1$	Log_{10} p(O_2)
none	-	1400	5	oxide liquid	0.10±0.00	47.2±0.1	52.7±0.1	-	Ox	-3.1	-11[C]
				$CaAl_2O_4^2$	0.02±0.02	35.0±0.1	65.0±0.1	-	Ox		
				metal	*99.98±0.05*	*0.01±0.01*	*0.01±0.04*	*-*	*Met*		
	-	1400	5	oxide liquid	0.18±0.03	47.3±0.3	52.5±0.2	-	Ox	-2.9	-10[C]
				$CaAl_2O_4^2$	0.70±0.08	33.8±0.2	65.5±0.3	-	Ox		
				metal	*99.99±0.01*	*0.01±0.00*	*0.00±0.00*	*-*	*Met*		
	-	1400	5	oxide liquid	0.30±0.06	47.4±0.3	52.3±0.2	-	Ox	-2.6	-9[C]
				$CaAl_2O_4^2$	0.12±0.00	35.3±0.0	64.6±0.0	-	Ox		
				metal	*99.98±0.00*	*0.02±0.02*	*0.00±0.01*	*-*	*Met*		
	-	1400	5	oxide liquid	0.82±0.39	46.9±0.4	52.2±0.2	-	Ox	-2.2	-8[C]
				$CaAl_2O_4^2$	0.07±0.00	36.7±0.0	63.2±0.0	-	Ox		
				metal	*99.98±0.02*	*0.02±0.03*	*0.00±0.01*	*-*	*Met*		
	-	1400	5	oxide liquid	1.0±0.2	47.1±0.3	51.9±0.2	-	Ox	-2.1	-7[C]
				$CaAl_2O_4^2$	0.12±0.03	35.1±0.0	64.8±0.1	-	Ox		
				metal	*99.96±0.00*	*0.01±0.00*	*0.03±0.00*	*-*	*Met*		
	-	1400	5	oxide liquid	1.8±0.3	46.4±0.3	51.8±0.2	-	Ox	-1.8	-6[C]
				$CaAl_2O_4^2$	0.18±0.00	35.1±0.1	64.7±0.1	-	Ox		
				metal	*99.97±0.02*	*0.03±0.02*	*0.00±0.00*	*-*	*Met*		
	-	1400	4	oxide liquid	2.2±0.2	46.0±0.1	51.9±0.1	-	Ox	-1.8	-6[C]
				$CaAl_2O_4^2$	0.23±0.05	35.2±0.1	64.5±0.1	-	Ox		
				metal	*99.81±0.07*	*0.13±0.08*	*0.07±0.01*	*-*	*Met*		
	-	1400	5	oxide liquid	3.4±0.6	45.2±0.5	51.4±0.2	-	Ox	-1.6	-5[C]
				$CaAl_2O_4^2$	0.08±0.04	36.5±0.2	63.4±0.1	-	Ox		
				metal	*99.94±0.2*	*0.02±0.04*	*0.04±0.05*	*-*	*Met*		
	-	1400	4	oxide liquid	6.4±0.1	43.0±0.2	50.6±0.1	-	Ox	-1.3	-4.5[C]
				$CaAl_2O_4^2$	0.13±0.05	35.1±0.1	64.8±0.1	-	Ox		
				metal	*99.96±0.03*	*0.01±0.00*	*0.03±0.03*	*-*	*Met*		
PbO/*Pb*	1450	1400	16	oxide liquid	1.6±0.2	46.5±0.2	51.6±0.1	0.23±0.07	Ox	-1.4	-6.5[E]
				$CaAl_2O_4^2$	0.06±0.02	35.0±0.1	64.9±0.1	0.04±0.00	Ox		
				metal	*95.0±0.7*	*0.03±0.01*	*0.01±0.02*	*5.0±0.7*	*Met*		
	-	1400	16	oxide liquid	5.9±0.1	43.8±0.1	50.2±0.2	0.15±0.08	Ox	-0.3	-4.4[E]
				$CaAl_2O_4^2$	0.16±0.01	35.1±0.3	64.6±0.5	0.22±0.22	Ox		
				metal	*99.70±0.13*	*0.01±0.02*	*0.02±0.02*	*0.26±0.13*	*Met*		
ZnO/*Zn*	1450	1400	16	oxide liquid	1.2±0.1	45.7±0.1	52.2±0.1	0.89±0.05	Ox	0.7	-7[E]
				$CaAl_2O_4^2$	0.00±0.00	34.7±0.0	65.3±0.0	0.00±0.00	Ox		
				metal	*99.79±0.08*	*0.02±0.01*	*0.02±0.02*	*0.17±0.06*	*Met*		
FeO/*Fe*	-	1400	5	oxide liquid	0.08±0.05	46.2±0.2	51.0±0.2	2.7±0.1	Ox	0.1	-11[C]
				$CaAl_2O_4^2$	0.03±0.03	35.4±0.2	64.4±0.2	0.15±0.04	Ox		
				metal	*98.3±0.1*	*0.01±0.01*	*0.01±0.02*	*1.7±0.1*	*Met*		
	-	1400	5	oxide liquid	0.32±0.05	42.6±0.2	48.6±0.2	8.4±0.1	Ox	1.3	-9[C]
				$CaAl_2O_4^2$	0.02±0.03	34.7±0.2	64.6±0.2	0.63±0.04	Ox		
				metal	*99.60±0.05*	*0.02±0.02*	*0.02±0.02*	*0.36±0.04*	*Met*		
$AsO_{1.5}$/*As*	-	1400	16	oxide liquid	2.7±0.1	45.9±0.2	50.5±0.1	0.88±0.06	Ox	-0.4	-5.6[E]
				$CaAl_2O_4^2$	0.07±0.00	34.7±0.2	65.2±0.2	0.00±0.00	Ox		
				metal	*98.6±0.3*	*0.02±0.02*	*0.04±0.05*	*1.4±0.3*	*Met*		
	1450	1400	16	oxide liquid	3.7±0.1	45.1±0.1	49.9±0.1	1.4±0.1	Ox	0.1	-5.1[E]
				$CaAl_2O_4^2$	0.12±0.08	34.8±0.1	65.1±0.1	0.00±0.00	Ox		

System	1450	1400	16	phase						L	$p(O_2)$
				metal	*99.12±0.06*	*0.02±0.01*	*0.01±0.01*	*0.85±0.06*	*Met*		
	1450	1400	16	oxide liquid	4.3±0.1	44.8±0.1	48.7±0.1	2.2±0.1	Ox	0.4	-4.9[E]
				$CaAl_2O_4$[2]	0.09±0.01	34.9±0.1	65.0±0.1	0.00±0.00	Ox		
				metal	*99.07±0.38*	*0.13±0.23*	*0.02±0.01*	*0.79±0.16*	*Met*		
SnO_2/*Sn*	1450	1400	16	oxide liquid	1.3±0.0	46.8±0.1	51.6±0.1	0.26±0.02	Ox	-0.8	-6.8[E]
				$CaAl_2O_4$[2]	0.06±0.02	34.9±0.1	65.0±0.1	0.00±0.00	Ox		
				metal	*98.9±0.1*	*0.01±0.01*	*0.01±0.01*	*1.0±0.1*	*Met*		
	1450	1400	16	oxide liquid	2.6±0.0	45.8±0.2	50.9±0.2	0.76±0.04	Ox	0.2	-5.7[E]
				$CaAl_2O_4$[2]	0.04±0.03	35.2±0.1	64.8±0.1	0.02±0.02	Ox		
				metal	*99.56±0.19*	*0.01±0.01*	*0±0.03*	*0.43±0.21*	*Met*		
	1450	1400	16	oxide liquid	4.4±0.2	43.6±0.1	50.5±0.1	1.5±0.1	Ox	1.0	-4.8[E]
				$CaAl_2O_4$[2]	0.05±0.04	34.8±0.0	65.1±0	0.02±0.03	Ox		
				metal	*99.85±0.06*	*0.01±0.01*	*0.01±0.02*	*0.13±0.07*	*Met*		
$SbO_{1.5}$/*Sb*	-	1400	16	oxide liquid	2.1±0.3	45.4±0.2	50.9±0.2	1.6±0.1	Ox	-1.0	-6.0[E]
				$CaAl_2O_4$[2]	0.07±0.08	34.8±0.0	65.1±0.1	0.02±0.03	Ox		
				metal	*89.0±1.4*	*0.01±0.01*	*0.01±0.02*	*11.0±1.4*	*Met*		
	-	1400	16	oxide liquid	3.4±0.1	44.6±0.1	48.2±0.2	3.9±0.1	Ox	-0.5	-5.2[E]
				$CaAl_2O_4$[2]	0.16±0.02	35.3±0.1	64.6±0.1	0.00±0.00	Ox		
				metal	*90.0±3.2*	*0.03±0.02*	*0.01±0.02*	*9.9±3.2*	*Met*		
$BiO_{1.5}$/*Bi*	-	1400	16	oxide liquid	4.0±0.2	45.1±0.2	50.8±0.1	0.08±0.03	Ox	-1.7	-5.0[E]
				$CaAl_2O_4$[2]	0.05±0.05	35.0±0.1	65.0±0.1	0.03±0.04	Ox		
				metal	*96.9±0.5*	*0.06±0.18*	*0.03±0.1*	*3.0±0.4*	*Met*		
	-	1400	16	oxide liquid	5.5±0.1	43.6±0.2	50.8±0.1	0.02±0.04	Ox	-1.2	-4.5[E]
				$CaAl_2O_4$[2]	0.16±0.02	34.7±0.1	65.1±0.1	0.02±0.04	Ox		
				metal	*99.69±0.10*	*0.02±0.01*	*0.04±0.05*	*0.26±0.1*	*Met*		
NiO/*Ni*	-	1400	16	oxide liquid	0.81±0.08	47.4±0.1	51.6±0.1	0.2±0.05	Ox	-1.7	-7.6[E]
				$CaAl_2O_4$[2]	0.04±0.03	35.4±0.0	64.6±0.0	0.03±0.03	Ox		
				metal	*93.7±0.4*	*0.01±0.01*	*0.03±0.03*	*6.3±0.4*	*Met*		
	-	1400	16	oxide liquid	1.7±0.1	45.8±0.1	51.8±0.1	0.64±0.05	Ox	-1.1	-6.4[E]
				$CaAl_2O_4$[2]	0.06±0.06	34.8±0.0	65.1±0.1	0.00±0.00	Ox		
				metal	*94.9±0.2*	*0.01±0.01*	*0.02±0.02*	*5.1±0.2*	*Met*		
	1450	1400	16	oxide liquid	3.7±0.1	43.8±0.1	50.4±0.1	2.1±0.1	Ox	-0.5	-5.1[E]
				$CaAl_2O_4$[2]	0.07±0.03	34.9±0.1	64.9±0.1	0.07±0.02	Ox		
				metal	*95.6±0.5*	*0.00±0.00*	*0.01±0.01*	*4.4±0.5*	*Met*		

[1]- for "$CuO_{0.5}$"-CaO-$AlO_{1.5}$ only system: L = wt.%$Cu_{oxide\ liquid}$/wt.%Cu_{metal} = wt.fr.$Cu_{oxide\ liquid}$
   for the system with Pb, Zn, Fe, As, Sn, Sb, Bi, Ni – L = wt.%$Me_{oxide\ liquid}$/wt.%Me_{metal}, where Me = [Pb, Zn, Fe, As, Sn, Sb, Bi, Ni].
[2]- the measurement of the phase composition was affected by secondary X-ray fluorescence and close presence of other phases
[E]- $p(O_2)$ over the system was estimated using the established correction (eq.1)
[C]- $p(O_2)$ over the system was controlled during the experiment
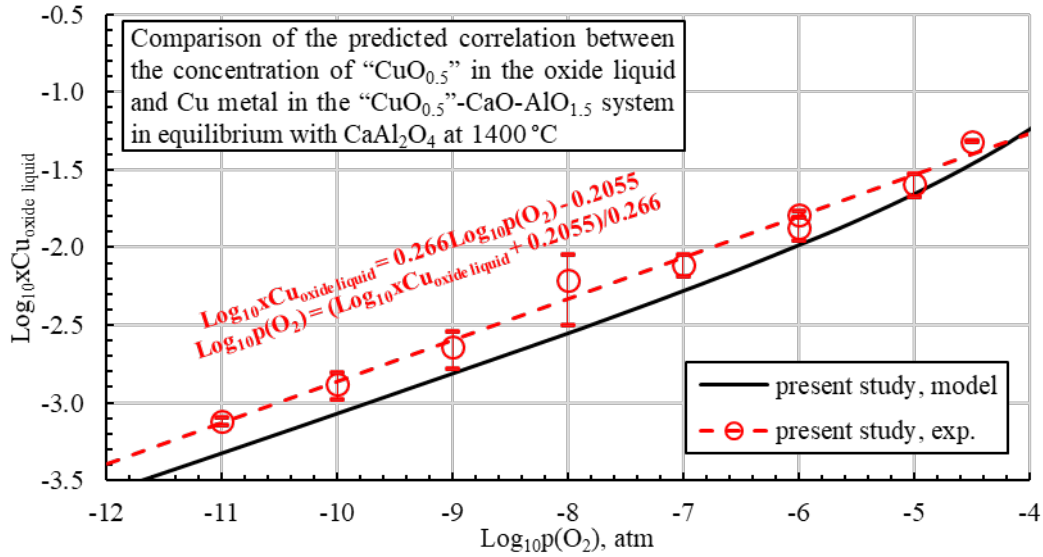
Figure 2. Comparison of the experimental correlation between the solubility of Cu in the oxide liquid of the "$CuO_{0.5}$"-CaO-$AlO_{1.5}$ system in equilibrium with Cu metal with the corresponding thermodynamic predictions (Shevchenko et al., 2021, Shishin et al., 2018, Shishin et al., 2019). In Y-axis, "xCu" is the molar ratio "$CuO_{0.5}$"/("$CuO_{0.5}$"+CaO+$AlO_{1.5}$).

The presented comparison indicates that the solubility of Cu at the described conditions is underestimated by the internal thermodynamic database (Shevchenko et al., 2021, Shishin et al., 2018, Shishin et al., 2019) and should be corrected in the future studies to comply with the recent experimental findings. Based on the obtained experimental results, the following equation was introduced to calculate the effective $p(O_2)$ over the system based on the concentration of "$CuO_{0.5}$" in the oxide liquid in equilibrium with Cu metal and $CaAl_2O_4$ solid:

$$Log_{10}p(O_2)_{estimated} = (Log_{10}xCu_{oxide\ liquid} + 0.2055)/0.266 \qquad (9)$$

Examples of typical microstructures observed in the studied samples were given in Figure 3. These micrographs were obtained using backscattered electron microscopy (BSE) to provide compositional contrast based on the mean atomic number. Figure 3a demonstrates phase equilibria among oxide liquid, $CaAl_2O_4$ and metallic phase, representing the microstructure of most of the samples presented in Table 1 and Figure 3b shows oxide liquid, $CaAl_2O_4$ and the metallic phase equilibrium in the part of the sample close to the Al_2O_3 crucible, demonstrating the isolation of the Al_2O_3 crucible by the consequently growing calcium aluminates, preventing further dissolution of the substrate into the melt.
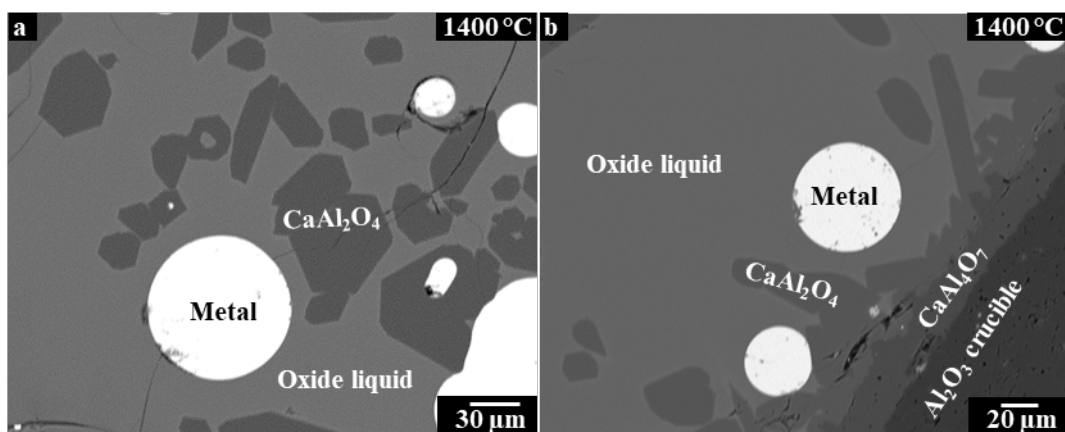
Figure 3. Examples of backscattered SEM micrographs of the quenched "$CuO_{0.5}$"-CaO-$AlO_{1.5}$-(Pb, Zn, Fe, As, Sn, Sb, Bi and Ni) samples in equilibrium with metal phase: (a) oxide liquid-$CaAl_2O_4$-metal (b) oxide liquid-$CaAl_2O_4$-metal, demonstrating isolation of the Al_2O_3 crucible with consequently forming layers of calcium aluminates.

The results for the experiments in the "$CuO_{0.5}$"-CaO-$AlO_{1.5}$-(Pb, Zn, Fe, As, Sn, Sb, Bi and Ni) system in equilibrium with metallic phase were given in Table 1. The experimental findings were graphically compared with the thermodynamic predictions for the distribution of the selected elements among the oxide liquid and metallic phases calculated using the FactSage software (Bale et al., 2016) and internal thermodynamic database (Shevchenko et al., 2021, Shishin et al., 2018, Shishin et al., 2019) in Figure 4.

It can be seen from Figure 4 that the predictions of the internal database (Shevchenko et al., 2021, Shishin et al., 2018, Shishin et al., 2019) for some of the elements such as Fe, Zn, Sb and Bi are in a great agreement with the experimental results. At the same time predictions for Sn, As, Ni and Cu are in a moderate agreement with the experiment. The predictions for the distribution of Pb were found to be inconsistent with the experimental findings and overestimated by an order of magnitude.
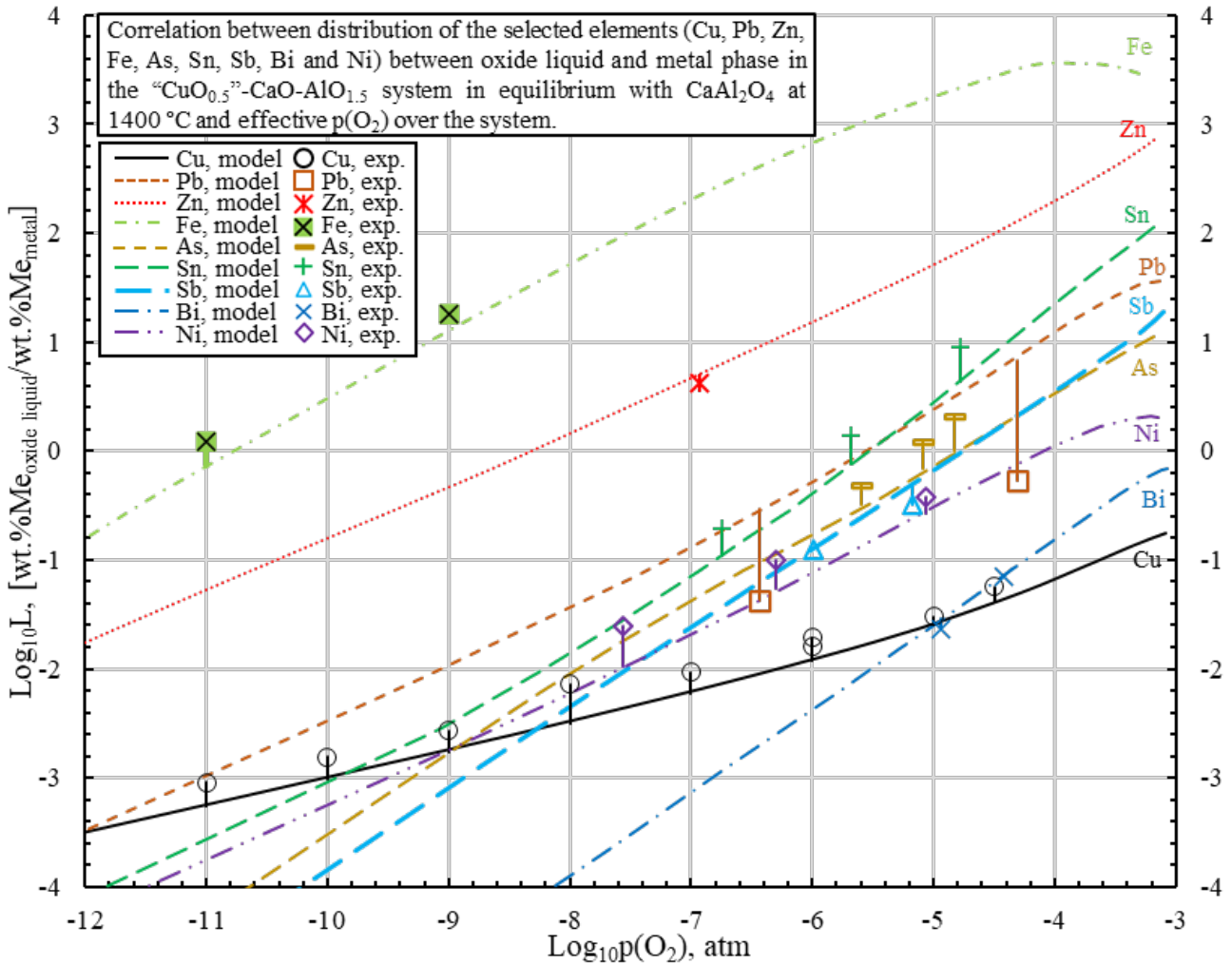
Figure 4. Comparison of the experimental correlation between the distribution of the selected elements (Cu, Pb, Zn, Fe, As, Sn, Sb, Bi and Ni) between oxide liquid and metal phase in the "CuO$_{0.5}$"-CaO-AlO$_{1.5}$ system in equilibrium with CaAl$_2$O$_4$ and effective p(O$_2$) over the system. In Y-axis, "L" is the distribution coefficient [wt.%Me$_{oxide\ liquid}$/wt.%Me$_{metal}$].

The outlined disagreements between the experimental results and the model predictions are to be corrected in the future studies during the systematic revision and reoptimisation of the Cu-Pb-Zn-Fe-Ca-Si-Al-Mg-O-S-(As, Sn, Sb, Bi, Ag, Au, Ni, Cr, Co and Na) gas/ oxide liquid/ matte/ speiss/ metal/ solids system. The results presented for the distribution of the selected elements between the oxide liquid and metallic phases of the "CuO$_{0.5}$"-CaO-AlO$_{1.5}$ system can be used as a powerful "diagnostic" tool to outline inconsistencies among selected binary, ternary and quaternary systems during the process of the model parameters optimisation.

CONCLUSIONS

Experimental data on the distribution of the Cu, Pb, Zn, Fe, As, Sn, Sb, Bi and Ni among the oxide liquid and the metallic phase in the "CuO$_{0.5}$"-CaO-AlO$_{1.5}$ system were obtained for the first time. Concentration of copper oxide in the "CuO$_{0.5}$"-CaO-AlO$_{1.5}$ oxide liquid in equilibrium with CaAl$_2$O$_4$ at 1400 °C was measured as a function of effective oxygen partial pressure (p(O$_2$)) over the system. The distributions of the Cu, Pb, Zn, Fe, As, Sn, Sb, Bi and Ni among the oxide liquid and the metallic phase in the "CuO$_{0.5}$"-CaO-AlO$_{1.5}$ system were obtained in the wide range of oxygen partial pressures from 10^{-11} to 10$^{-3.7}$.

The experimental results were compared to the existing thermodynamic predictions to outline areas of inconsistency to be corrected in the future studies devoted to the systematic revision and reoptimisation of the Cu-Pb-Zn-Fe-Ca-Si-Al-Mg-O-S-(As, Sn, Sb, Bi, Ag, Au, Ni, Cr, Co and Na) gas/oxide liquid/matte/speiss/metal/solids system.

ACKNOWLEDGEMENTS

REFERENCES

ANINDYA, A., SWINBOURNE, D., REUTER, M. & MATUSEWICZ, R. 2013. Distribution of elements between copper and FeOx –CaO–SiO2 slags during pyrometallurgical processing of WEEE Part 1 – Tin. *Mineral Processing and Extractive Metallurgy IMM Transactions section C, 122, 165-173*

ANINDYA, A., SWINBOURNE, D., REUTER, M. & MATUSEWICZ, R. 2014. Distribution of elements between copper and FeOx –CaO–SiO2 slags during pyroprocessing of WEEE Part 2 – Indium. *Mineral Processing and Extractive Metallurgy (Trans. Inst. Min Metall. C)*, 123, 43-52

BALE, C. W., BELISLE, E., CHARTRAND, P., DECTEROV, S. A., ERIKSSON, G., GHERIBI, A. E., HACK, K., JUNG, I. H., KANG, Y. B., MELANCON, J., PELTON, A. D., PETERSEN, S., ROBELIN, C., SANGSTER, J., SPENCER, P. & VAN ENDE, M. A. 2016. FactSage thermochemical software and databases, 2010-2016. *CALPHAD,* 54**,** 35-53.

BALE, C. W., BÉLISLE, E., CHARTRAND, P., DECTEROV, S. A., ERIKSSON, G., HACK, K., JUNG, I. H., KANG, Y. B., MELANÇON, J., PELTON, A. D., ROBELIN, C. & PETERSEN, S. 2009. FactSage thermochemical software and databases — recent developments. *Calphad,* 33**,** 295-311.

CHEN, M., AVARMAA, K., KLEMETTINEN, L., SHI, J., TASKINEN, P. & JOKILAAKSO, A. 2020. Experimental Study on the Phase Equilibrium of Copper Matte and Silica-Saturated FeO$_x$-SiO$_2$-Based Slags in Pyrometallurgical WEEE Processing. *Metall. Mater. Trans. B,* 51**,** 1552-1563.

DUNCUMB, P. 1971. Quantitative electron probe microanalysis. *Electron Microsc. Anal., Proc. Anniv. Meet., 25th,* 132-137.

DUNCUMB, P. & REED, S. J. B. 1968. Calculation of stopping power and backscatter effects in electron probe microanalysis. Tube Investments Res. Lab., Cambridge, UK.

FALLAH-MEHRJARDI, A., HIDAYAT, T., HAYES, P. C. & JAK, E. 2017. Experimental Investigation of Gas/Slag/Matte/Tridymite Equilibria in the Cu-Fe-O-S-Si system in Controlled Gas Atmospheres: Development of Technique. *Metall. Mater. Trans. B,* 48**,** 3002-3016.

HIDAYAT, T., CHEN, J., HAYES, P. C. & JAK, E. 2021. Distributions of As, Pb, Sn and Zn as minor elements between iron silicate slag and copper in equilibrium with tridymite in the Cu-Fe-O-Si system. *Int. J. Mater. Res.,* 112**,** 178-188.

HIDAYAT, T., HAYES, P. C. & JAK, E. 2018. Phase Equilibria in the ZnO-"FeO"-SiO$_2$ System in Reducing Atmosphere and in the ZnO-"FeO"-SiO$_2$-"Cu$_2$O" System in Equilibrium with Liquid Copper Metal at 1250 °C (1523 K). *Metall. Mater. Trans. B,* 49**,** 1766-1780.

HIDAYAT, T., HENAO, H. M., HAYES, P. C. & JAK, E. 2012. Phase Equilibria Studies of Cu-O-Si Systems in Equilibrium with Air and with Metallic Copper, and Cu-Me-O-Si Systems (Me = Ca, Mg, Al, and Fe) in Equilibrium with Metallic Copper. *Metall. Mater. Trans. B,* 43**,** 1290-1299.

JAK, E. 2012. Integrated experimental and thermodynamic modelling research methodology for metallurgical slags with examples in the copper production field *9th Intl. Conf. on Molten Slags, Fluxes and Salts.* Beijing, China: The Chinese Society for Metals, 1-28

JAK, E., HAYES, P. C. & LEE, H.-G. 1995. Improved methodologies for the determination of high temperature phase equilibria. *Korean Journal of Minerals and Materials Institute (Seoul),* 1**,** 1-8.

KHARTCYZOV, G., SHEVCHENKO, M., CHENG, S., HAYES, P. C. & JAK, E. 2022. Experimental phase equilibria studies in the "$CuO_{0.5}$"-CaO-SiO_2 ternary system in equilibrium with metallic copper. *Ceram. Int.,* 48**,** 9927-9938.

KHARTCYZOV, G., SHEVCHENKO, M., CHENG, S., HAYES, P. C. & JAK, E. 2023. Experimental phase equilibria study and thermodynamic modelling of the "CuO0.5"-AlO1.5-SiO2 ternary system in equilibrium with metallic copper. *Ceramics International,* 49**,** 11513-11528.

KLEMETTINEN, L., AVARMAA, K. & TASKINEN, P. 2017. Slag Chemistry of High-Alumina Iron Silicate Slags at 1300 C in WEEE Smelting. *J. Sustain. Metall, 772-781*

LOIBL, A. & TERCERO ESPINOZA, L. A. 2021. Current challenges in copper recycling: aligning insights from material flow analysis with technological research developments and industry issues in Europe and North America. *Resources, Conservation and Recycling,* 169**,** 105462.

LUTY, W. 1992. Types of Cooling Media and Their Properties. *In:* LIŠČIĆ, B., TENSI, H. M. & LUTY, W. (eds.) *Theory and Technology of Quenching: A Handbook.* Berlin, Heidelberg: Springer Berlin Heidelberg.

NAGAMORI, M. & MACKEY, P. J. 1977. Distribution Equilibriums of Tin, Selenium and Tellurium Between Iron(II) Oxide-Iron(III) Oxide-Silicon(IV) Oxide-Alumina-Copper Oxide ($CuO_{0.5}$) Slag and Metallic Copper. *Metall. Trans. B,* 8B**,** 39-46.

PHILIBERT, J. 1963. Method for calculating the absorption correction in electron-probe microanalysis. *X-Ray Opt. X-Ray Microanal., 3rd Intl. Symp., Stanford Univ.***,** 379-392.

PIZETTA ZORDÃO, L. H., OLIVEIRA, V. A., TOTTEN, G. E. & CANALE, L. C. F. 2019. Quenching power of aqueous salt solution. *Int. J. Heat Mass Transf.,* 140**,** 807-818.

SHEVCHENKO, M., CHEN, J. & JAK, E. Establishing additional correction for quantitative EPMA measurements in the system PbO-SiO_2. AMAS 2017, 14th Biennial Australian Microbeam Analysis Symposium, 6-10 February 2017 Brisbane, Australia. O-Pb-Si QUT, Brisbane, 94-95.

SHEVCHENKO, M., HIDAYAT, T., HAYES, P. & JAK, E. 2016. Liquidus of "FeO"-SiO_2-PbO slags in equilibrium with air and with metallic lead. *10th Intl. Conf. on Molten Slags, Fluxes and Salts.* Seattle, Washington, USA, 1221-1228

SHEVCHENKO, M. & JAK, E. 2017. Experimental Phase Equilibria Studies of the PbO-SiO_2 System. *J. Am. Ceram. Soc,* 101**,** 458-471.

SHEVCHENKO, M. & JAK, E. 2018. Experimental Liquidus Studies of the Pb-Fe-Si-O System in Equilibrium with Metallic Pb. *Metall. Mater. Trans. B,* 49**,** 159-180.

SHEVCHENKO, M. & JAK, E. 2019. Experimental Liquidus Studies of the Binary Pb-Cu-O and Ternary Pb-Cu-Si-O Systems in Equilibrium with Metallic Pb-Cu Alloys. *J. Phase Equilib. Diff.,* 40**,** 671–685.

SHEVCHENKO, M. & JAK, E. 2020. Experimental Liquidus Studies of the ZnO-"$CuO_{0.5}$" and ZnO-"$CuO_{0.5}$"-SiO_2 Liquidus in Equilibrium with Cu-Zn Metal. *J. Phase Equilib. Diff.,* 41**,** 207-217.

SHEVCHENKO, M., SHISHIN, D., HAYES, P. C. & JAK, E. Recent Developments in Experimental and Thermodynamic Modelling Techniques for the Characterisation of Phase Equilibria in Complex High Temperature Oxide Systems. The 11th International Conference on Molten Slags, Fluxes and Salts, 2021 Virtual, Korea.

SHISHIN, D., HAYES, P. & JAK, E. 2018. *Multicomponent Thermodynamic Databases for Complex Non-ferrous Pyrometallurgical Processes*, 853-868

SHISHIN, D., HAYES, P. & JAK, E. 2019. *DEVELOPMENT AND APPLICATIONS OF THERMODYNAMIC DATABASE IN COPPER SMELTING*, 1-13

YAZAWA, A. Extractive metallurgical chemistry with special reference to copper smelting. 28th Congress of IUPAC 1981 Vancouver. Cu-Fe-O-S-Si Ca-Fe-O-Si 1-21.